Supporting Information

Non-centrosymmetric Structures Designed Rationally by "Dimensionality Addition" Strategy toward Promising Nonlinear Optical Family [A-X][In-Se] (A = K/Ba, Rb/Ba; X = Cl, Br)

Shao-Min Pei,[a],[b] Fan Wu,[a] Ming-Shu Zhang,[a] Wen-Fa Chen,[a] Xiao-Ming Jiang,[a],[b] Bin-Wen Liu,[a],[b]*and Guo-Cong Guo[a],[b]*

[a] State Key Laboratory of Structural Chemistry, Fujian Institute of Research on the Structure of Matter, Chinese Academy of Sciences, Fuzhou, Fujian, 350002, P. R. China

[b] Fujian Science & Technology Innovation Laboratory for Optoelectronic Information of China, Fuzhou, Fujian 350002, P. R. China.

*E-mail address: gcguo@fjirsm.ac.cn (G.-C. Guo); bwliu@fjirsm.ac.cn (B.-W. Liu)

Table of Contents

Exerimental Section

Crystal Synthesis. Crystals **1**–**6** were synthesized via the conventional high-temperature solid-state reactions. For synthesizing compound **1**, firstly, accurately weighed the raw materials Sm (0.14 mmol), In (0.70 mmol), Se (1.25 mmol), and KCl (2.01 mmol) into a quartz tube. Vacuumed the quartz tube to 10^{-4} Torr and sealed it using a hydrogen-oxygen flame. Subsequently, placed the sealed tube in a temperature-controlled muffle furnace programmed with the following temperature profile: Ramped up from room temperature to 300°C over a period of 5 h; held at 300°C for 5 h; further ramped up to 850°C over another 5 h; maintained at this temperature for 96 h; then decreased to 550°C over a duration of 99 h; finally, cooled down to 350°C within approximately 66 h before terminating the procedure. After rinsing the product with deionized water, dark red blocky crystal **1** could be isolated. The preparation process for all other compounds remains identical to that described above except for variations in raw materials and temperature curves. The specific synthesis schemes of **2**–**6** are as follows:

$Rb[Rb_4Cl][In_{14}Se_{23}]$ (2). By replacing KCl in the feedstock of compound **1** with an equivalent amount of RbCl, and subsequently undergoing the identical reaction process as **1**, microcrystalline **2** could be obtained.

$K_2[K_3BaCl][In_{18}Se_{30}]$ (3). Quartz tubes loaded with Ba (0.23 mmol), In (1.38 mmol), Se (2.30 mmol), and KCl (0.38 mmol) were subjected to a high-temperature solid-phase reaction to afford microcrystalline **3** according to the following temperature profile: it rised from room temperature to 300°C in 5 h, then stayed at 300°C for 5 h, and then heated to 950 ° C in 10 h. After 4 days of holding, the temperature was reduced to 650°C after 99 h, and finally cooled down to 350 °C after the same period of time before stopping the programmed temperature control.

$Rb_2[Rb_3BaCl][In_{18}Se_{30}]$ (4). The raw materials utilized for the synthesis of microcrystalline **4** encompass: Ba (0.22 mmol), In (1.32 mmol), Se (2.20 mmol) and RbCl (0.37 mmol). Compound **4** could be acquired by employing an identical temperature program as that employed for **3**.

$[K_4Cl][LiK_{10}Cl_4][In_{22}Se_{38}]$ (5). The reaction feedstock for the crystal growth of compound **5** included Li (0.39 mmol), In (0.66 mmol), Se (1.19 mmol), LiCl (0.66 mmol), and KCl (2.28 mmol). The quartz tube with the above mixture was put into the muffle furnace and set up the following program: the heating process involved ramping up from room temperature to 300°C, followed by a period of constant temperature.The temperature then further rised to 600°C before entering another period of constant temperature. Each of the aforementioned sessions lasted 6 h. After completing the constant temperature phase at 600°C, there is a subsequent ramp-up to reach 900°C within a duration of 12 h. This elevated temperature is then sustained for a period of 4 days before gradually cooling down to 400°C over an additional span of 4 days, after which the power can be switched off.

$[K_4Cl][BaK_9Cl_4][In_{22}Se_{38}]$ (6). The raw material for crystal growth of compound **6** and their dosage were as follows: Ba (0.31 mmol), In (1.40 mmol), Se (2.49 mmol), and KCl (2.01 mmol). The heating route

of compound **6** was completely different from that of **5**: it underwent a gradual heating process over a duration of 6 h until reaching a temperature of 300°C, and maintained for a period of 12 h; subsequently, it further heated up to reach a maximum temperature of 700°C over another span of 12 h; following this stage, after being held at the elevated temperature for 4 day before gradually cooling down to 450°C over a period of 4 days; finally, it experienced cooling down to 300°C after 33h, at which point the power could be switched off.

Crystals **1–4** remained stable in air for a minimum of three months. In contrast, crystals **5** and **6** exhibited surface discoloration within approximately one week of air exposure. Following ultrasonic cleaning, the surface impurities were effectively removed, restoring their original luster. Single-crystal analysis confirmed that these crystals retained their initial structure without undergoing decomposition. Moreover, semiquantitative microprobe element analysis of **1**–**6** was proceeded by a Hitachi S-3500 SEM spectrometer equipped with energy-dispersive X-ray spectroscopy (EDS).

Single-crystal and powder XRD. The single-crystal XRD datasets of **1**–**6** were acquired at a temperature of 293 K using an advanced Rigaku FR-X microfocus diffractometer. The instrument was equipped with a graphite monochromatic Mo-$K\alpha$ radiation source (λ = 0.71073 Å). Initial atomic positions were determined using direct methods, and the structures were further refined employing the F^2 technique of full matrix least squares, incorporating anisotropic thermal parameters for individual atoms. All calculations were executed using the crystallography software package Siemens SHELXTL version 5.[1] It is worth noting that the significant residual electron density observed near the Ba atoms in compounds **3** and **4** can be attributed to the heavy-atom absorption effect of the Ba atoms. To conduct the powder XRD analysis of **1**–**6**, we utilized the Rigaku MiniFlex600 X-ray diffractometer that boasted a diffractive monochromator specifically designed for Cu $K\alpha$ radiation (λ = 1.54057 Å).

Infrared and UV−Vis−NIR Diffuse Reflectance Spectroscopy. The microcrystalline forms of **1**–**6** were subjected to infrared spectroscopy using a Nicolet Magana 750 FT-IR spectrophotometer, covering the wavenumber range of 4000−400 cm^{-1}. The UV-Vis-NIR diffuse reflectance spectra of **1**–**6** were obtained through recording with a Perkin-Elmer Lambda 900 UV-Vis spectrophotometer, spanning the wavelength range of 200−2500 nm. The samples were specifically tested in a flat position on a quartz glass plate with $BaSO_4$ serving as the substrate. The Kubelka-Munk formula, denoted as $F(R) = \alpha/S = (1-R)^2/2R$, was employed for the acquisition of absorption spectra.[2] Here, α represents the absorption coefficient, S denotes the scattering coefficient, and R signifies the reflectance.

SHG Measurements. An improved Kurtz-Perry method was utilized to evaluate the SHG intensities when exposed to an irradiation with a wavelength of 1910 nm.[3] Microcrystalline samples of **1**–**6** and AGS, ranging in particle sizes from 30−50, 50−75, 75−100, 100-150, 150−200 μm, were prepared for phase-matching measurements. Importantly, the benchmark AGS samples were acquired from a high-quality large-size crystal. The frequency-doubled signals at a wavelength of 955 nm were detected using Andor's DU420A-BR-DD charge-coupled device (CCD) camera.

Computation Procedure. Considering that the Se4/Se4A and Se5/Se5A atoms in compounds **4** are associated with fission disorder, only Se4 and Se5 were retained as structural component for the theoretical calculation. In addition, the disordered K1/Ba1 and K2/Ba2 sites in compound **6** must be converted into an ordered structure in MS prior to theoretical calculations. For instance, after eliminating the structural symmetry, 1/3 of the disordered K1/Ba1 positions are assigned as Ba1 atoms, while 2/3 are designated as K1 atoms. The bond valence s_i was calculated using $s_i = \exp[(R_o - R_i)/B]$,[4] where R_o and B are constants determined empirically for each type of bond, with the former being the notional length of a bond of unit valence and the latter a measure of the softness of the bond. These parameters were tabulated for most bond types by Brown. The COHP analysis was facilitated by the Lobster software in conjunction with VASP.[5] The electronic band structures and electron density difference were computationally determined using the CASTEP module within Materials Studio package, and their NLO properties were investigated using the *ABINIT* package, both of which are based on density functional theory (DFT).[6] We opted for the Perdew, Burke, and Ernzerfhof (PBE) parametrized generalized gradient approximation (GGA) as our choice for the exchange-correlation functional.[7] Valence configurations K-$3p^6 4s^1$, Rb-$4p^6 5s^1$, Ba-$6s^2 5p^6$, Li-$2s^1$, In-$4d^{10} 5s^2 5p^1$, Se-$4s^2 4p^4$, and Cl-$3s^2 3p^5$ were employed in conjunction with projector-augmented plane-wave pseudopotentials.[8] The energy cut-off for plane-wave was set at 18 Hartree. The the linear optical properties were determined by calculating the complex dielectric function $\varepsilon_{ij,re} = \varepsilon_{ij,re}(\omega) + \varepsilon_{ij,im}(\omega)$, which was achieved using the expression $\frac{4\pi}{\Omega}\sum_{nmk} f_{nm}(k)\frac{r^{i}_{nm}(k) r^{j}_{mn}(k)}{\omega_{mn}(k) - \omega} + \delta_{ij}$, where $\varepsilon_{re}(\omega)$ represents real part while $\varepsilon_{im}(\omega)$ represents imaginary part of the dielectric function. Relevant calculations also took into account the matrix elements $r^{i}_{nm}(k)$ associated with states. In addition, the DFT and "sum over states" methods were utilized to assess frequency-dependent SHG susceptibility tensors $\chi_{ijk}(2\omega, \omega, \omega)$. It is important to mention that the SHG susceptibility comprises three components: a pure inter-band transition term denoted as χ_{inter} $(2\omega, \omega, \omega)$; an intra-band transition term described as χ_{intra} $(2\omega, \omega, \omega)$ which accounts for the modulation of linear susceptibility by electron intra-band motion; and a modulation term represented by χ_{mod} $(2\omega, \omega, \omega)$ that considers intra-band contribution influenced by motion-related polarization energy.[9]

Figures and Tables

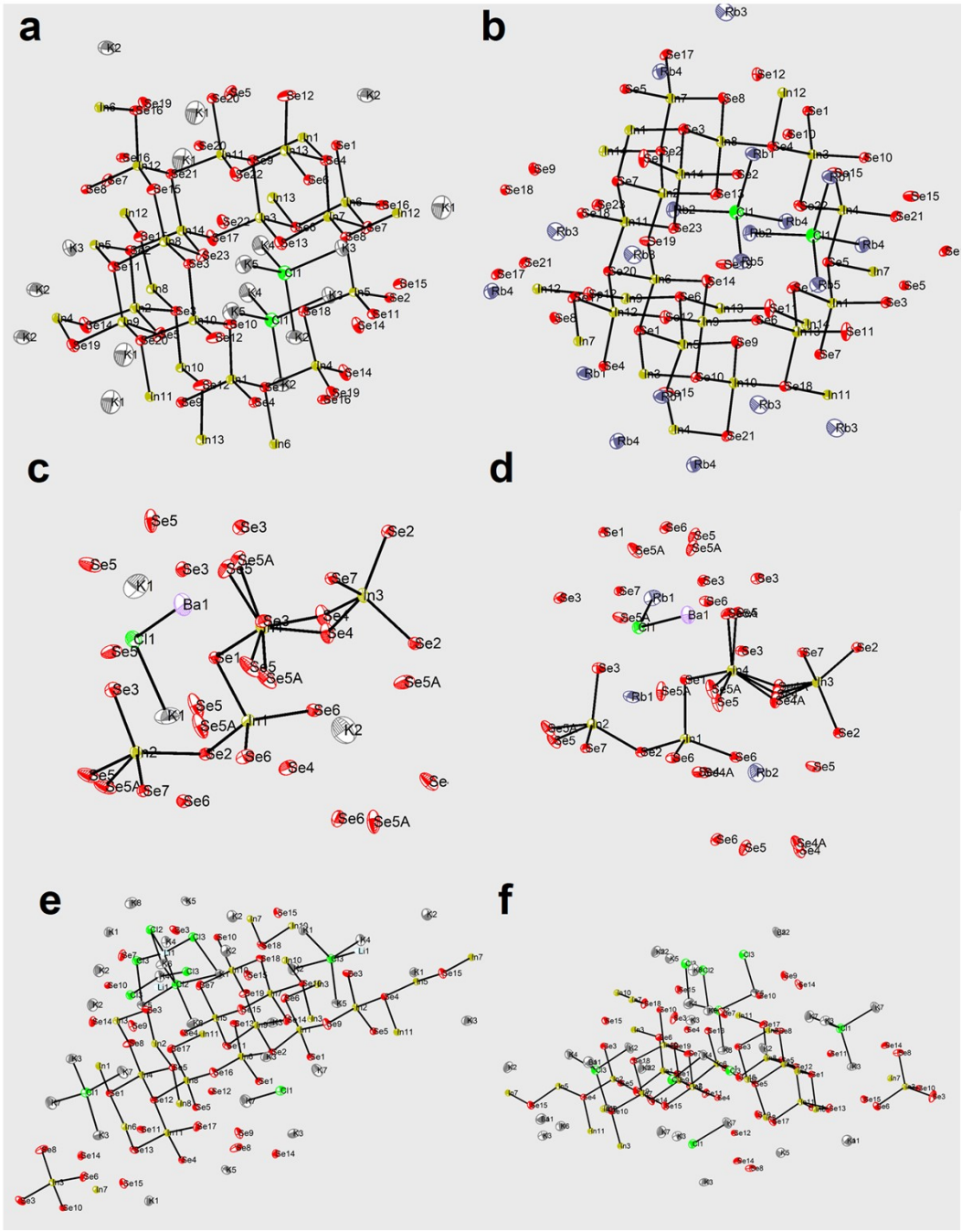

Fig. S1 Ortep plots of **1** (a), **2** (b), **3** (c), **4** (d), **5** (e), and **6** (f).

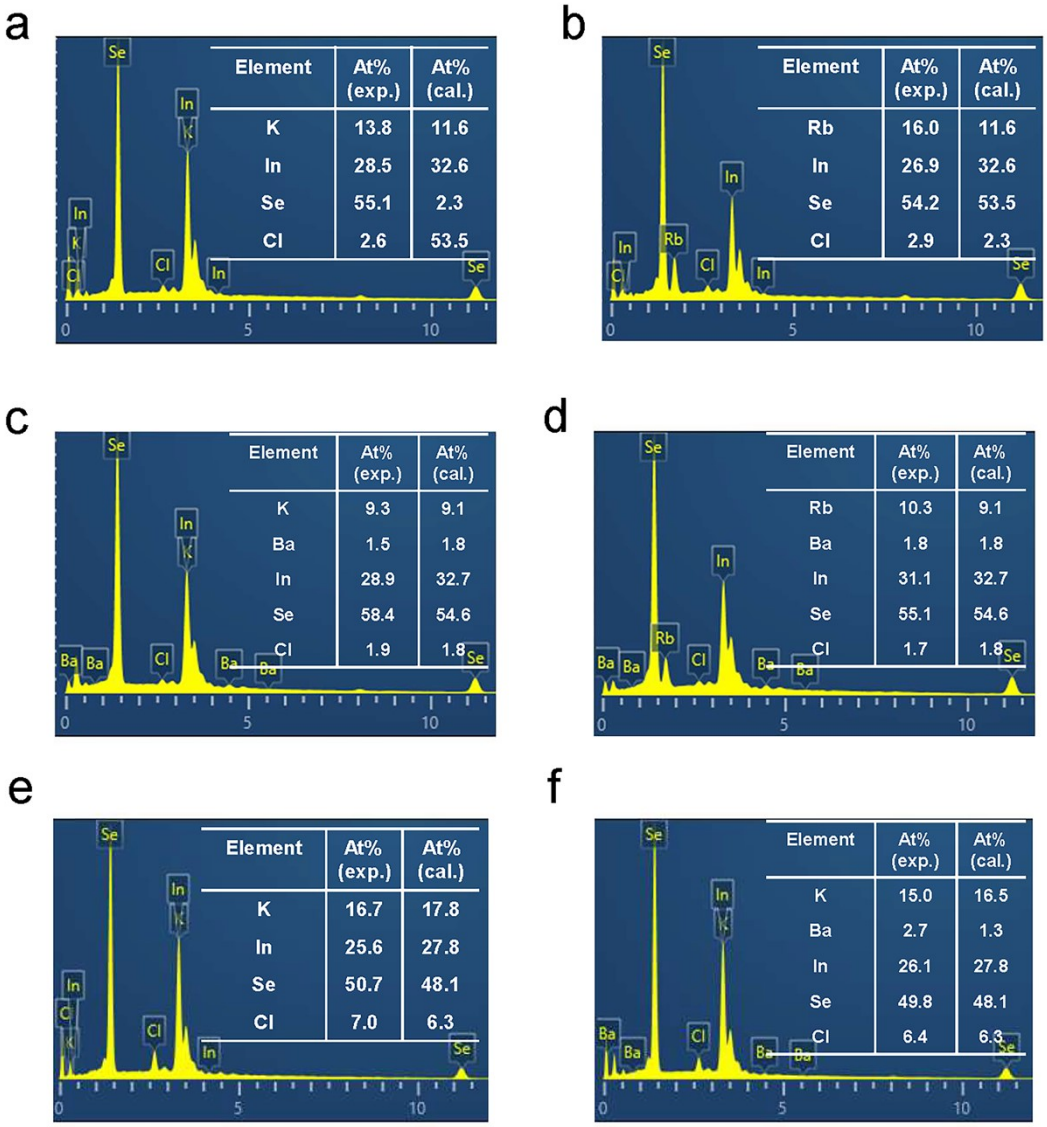

Fig. S2 The EDS results of **1** (a), **2** (b), **3** (c), **4** (d), **5** (e), **6** (f).

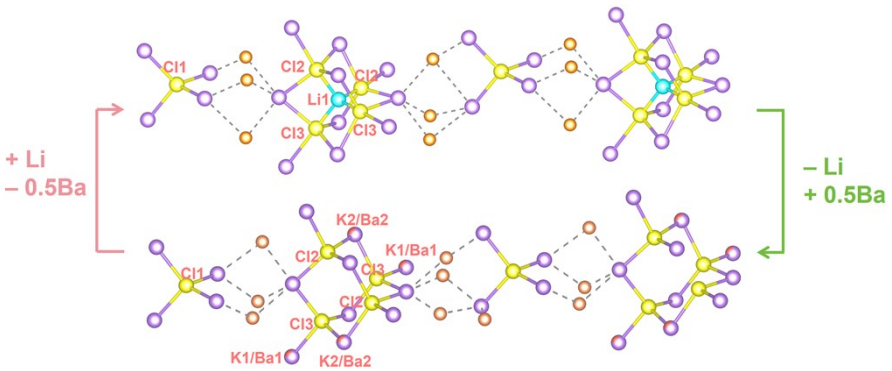

Fig. S3 Structural transformation of dual polycations in **5** (up) and **6** (down).

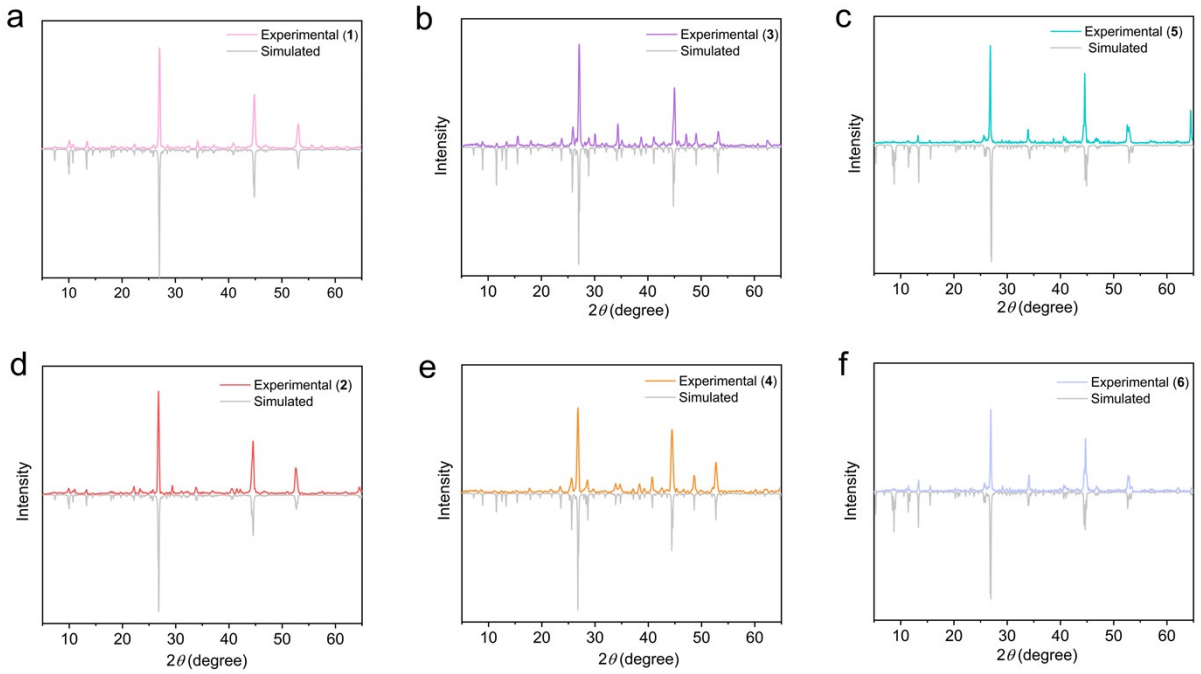

Fig. S4 The experimental and simulated XRD patterns of **1** (a), **2** (d), **3** (b), **4** (e), **5** (c), **6** (f).

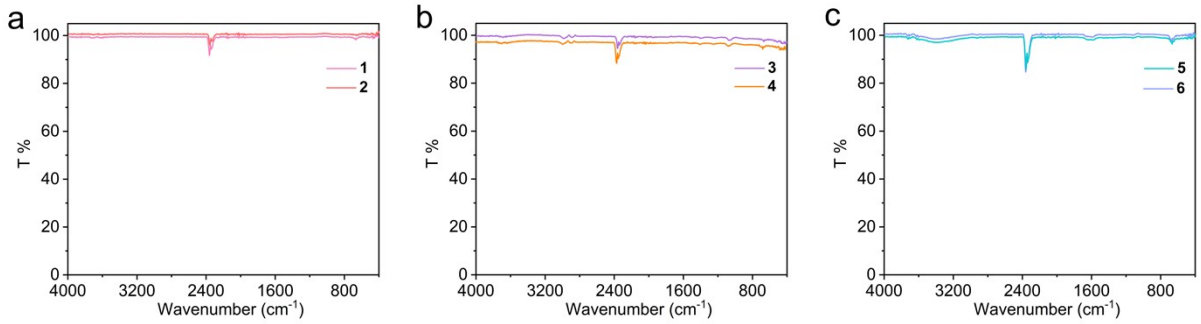

Fig. S5 The infrared spectra of **1** and **2** (a), **3** and 4 (b), **5** and **6** (c).

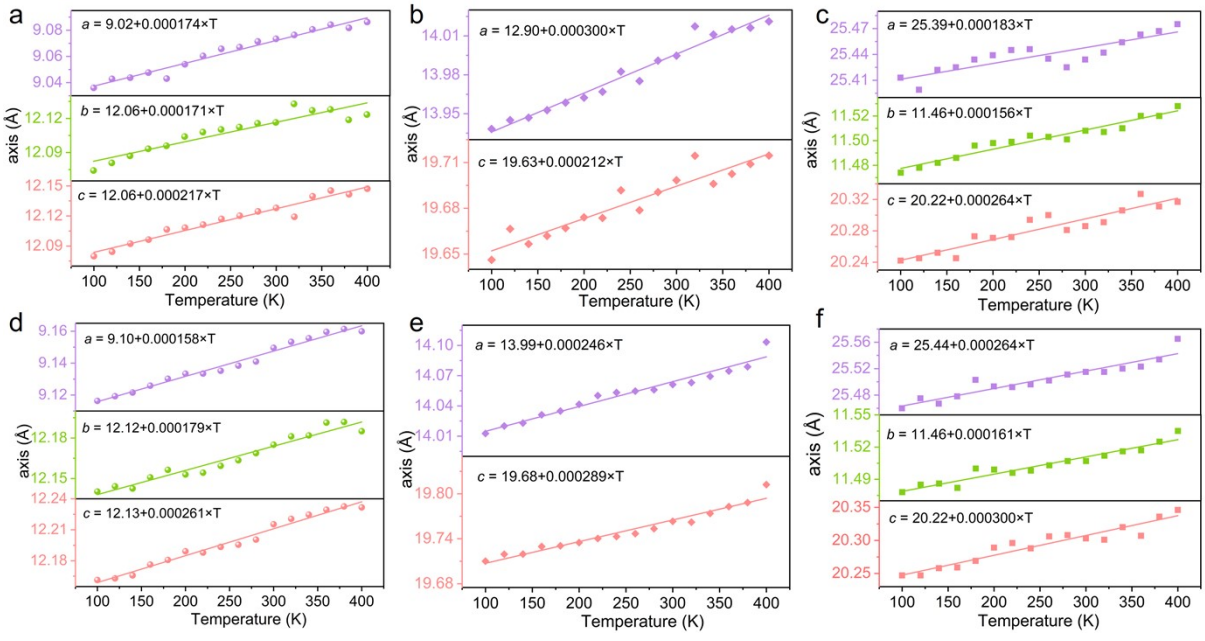

Fig. S6 Variable-temperature lattice parameters of *a*-, *b*-, and *c*-axes in **1** (a), **2** (d), **3** (b), **4** (e), **5** (c), **6** (f).

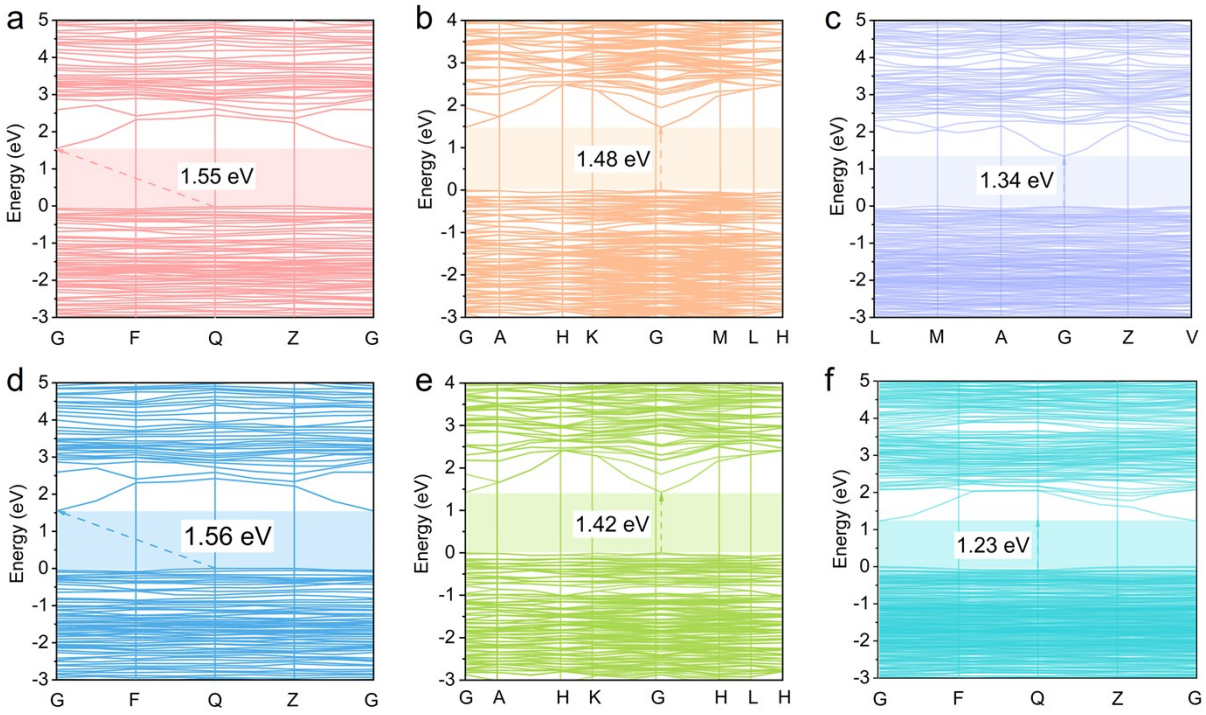

Fig. S7 Electronic band structures of **1** (a), **2** (d), **3** (b), **4** (e), **5** (c), and **6** (f).

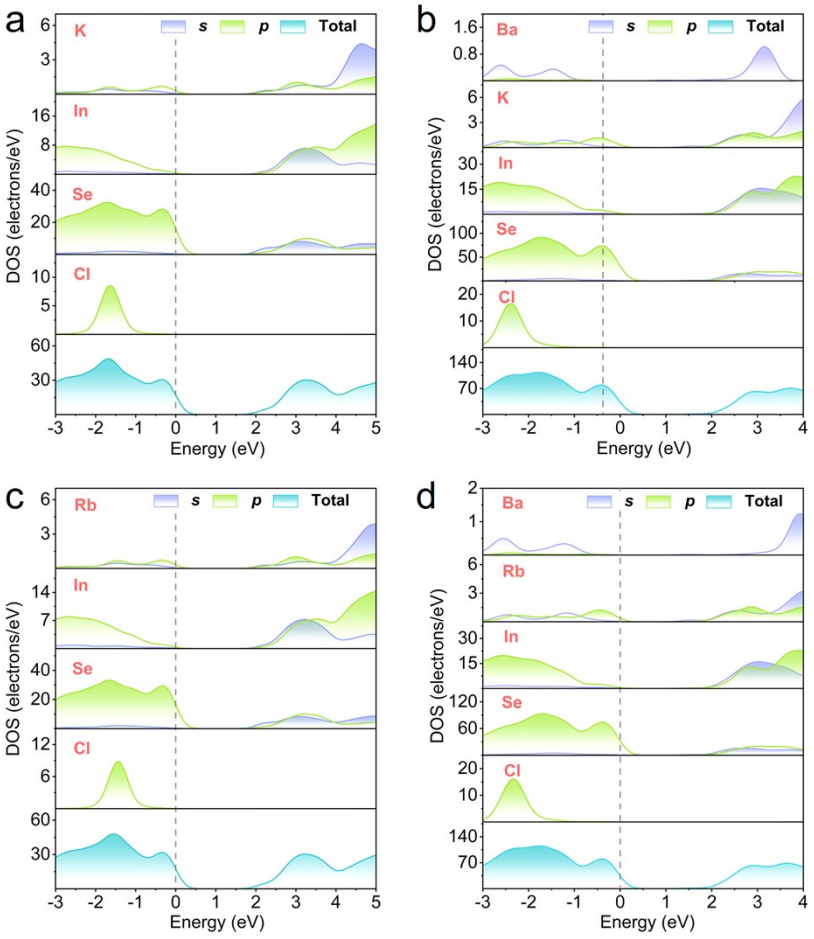

Fig. S8 Density of states (DOS) of **1** (a), **2** (c), **3** (b), and **4** (d).

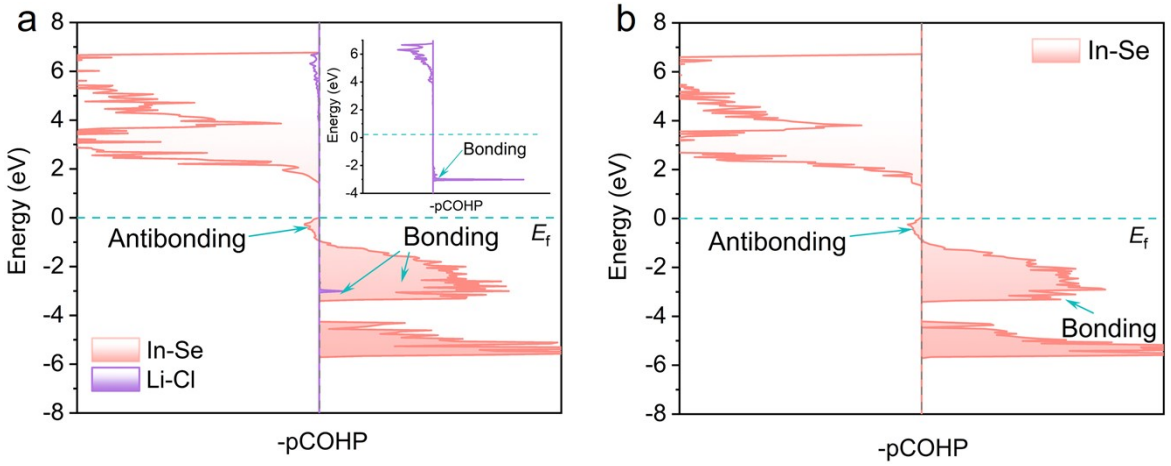

Fig. S9 partial COHP curves of In-Se and Li-Cl pairs in **5** (a), In-Se pairs in **6** (b).

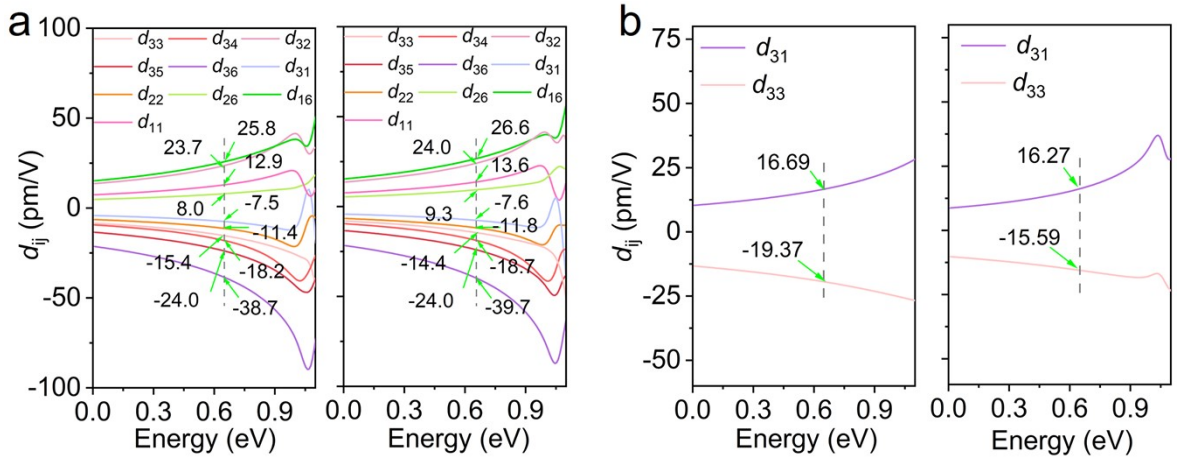

Fig. S10 calculated frequency-dependent SHG tensors of **1** and **2** (a), **3** and **4** (b).

Table S1. Crystallographic data and structure refinement parameters for **1**–**6**.

Empirical formula	$K[K_4Cl][In_{14}Se_{23}]$ (**1**)	$Rb[Rb_4Cl][In_{14}Se_{23}]$ (**2**)
CSD	2371874	2371875
Fw	3654.51	3886.36
Temperature (K)	293(2)	293(2)
Space group	*P*1	*P*1
a (Å)	9.0671(2)	9.14260(10)
b (Å)	12.1162(3)	12.1760(2)
c (Å)	12.1238(3)	12.2109(2)
α (°)	93.193(2)	93.2310(10)
β (°)	94.436(2)	94.4960(10)
γ (°)	98.838(2)	98.8540(10)
V (Å^3)	1309.06(5)	1335.76(3)
Z	1	1
D_{calcd} (g cm^{-3})	4.636	4.831

μ (mm^{-1})	22.480	26.167
GOF on F^2	0.888	1.026
$R_1{}^a$ ($I > 2\sigma$ (I))	0.0285	0.0283
$wR_2{}^b$ ($I > 2\sigma$ (I))	0.0576	0.0662
$R_1{}^a$ (all data)	0.0341	0.0299
$wR_2{}^b$ (all data)	0.0600	0.0669
$\Delta\rho_{max}/\Delta\rho_{min,}$ (e Å^{-3})	0.81/−0.67	1.09/−1.00
Flack	0.021(7)	0.001(6)
Empirical formula	$K_2[K_3BaCl][In_{18}Se_{30}]$ (**3**)	$Rb_2[Rb_3BaCl][In_{18}Se_{30}]$ (**4**)
CSD	2371878	2371877
Fw	4803.85	5035.70
Temperature (K)	293(2)	293(2)
Space group	$P6_3cm$	$P6_3cm$
a (Å)	14.0037(3)	14.06810(10)
b (Å)	14.0037(3)	14.06810(10)
c (Å)	19.6844(9)	19.7774(2)
α (°)	90	90
β (°)	90	90
γ (°)	120	120
V (Å^3)	3343.0(2)	3389.77(6)
Z	2	2
D_{calcd} (g cm^{-3})	4.772	4.934
μ (mm^{-1})	23.345	26.283
GOF on F^2	1.057	1.088
$R_1{}^a$ ($I > 2\sigma$ (I))	0.0207	0.0197
$wR_2{}^b$ ($I > 2\sigma$ (I))	0.0425	0.0496
$R_1{}^a$ (all data)	0.0239	0.0203
$wR_2{}^b$ (all data)	0.0433	0.0499
$\Delta\rho_{max}/\Delta\rho_{min,}$ (e Å^{-3})	0.99/−1.95	1.61/−1.57
Flack	0.046(14)	0.024(9)
Empirical formula	$[K_4Cl][LiK_{10}Cl_4][In_{22}Se_{38}]$ (**5**)	$[K_4Cl][BaK_9Cl_4][In_{22}Se_{38}]$ (**6**)
CSD	2371881	2371879
Fw	6258.11	6349.41
Temperature (K)	293(2)	293(2)
Space group	C2	C2
a (Å)	25.4344(14)	25.552(5)
b (Å)	11.4919(3)	11.5176(3)
c (Å)	20.2696(19)	20.3164(19)
α (°)	90	90
β (°)	125.124(9)	125.12(2)
γ (°)	90	90
V (Å^3)	4845.8(7)	4890.7(15)
Z	2	2
D_{calcd} (g cm^{-3})	4.289	4.312
μ (mm^{-1})	20.147	20.313
GOF on F^2	1.003	1.022
$R_1{}^a$ ($I > 2\sigma$ (I))	0.0261	0.0490
$wR_2{}^b$ ($I > 2\sigma$ (I))	0.0514	0.1252
$R_1{}^a$ (all data)	0.0317	0.0555
$wR_2{}^b$ (all data)	0.0531	0.1290
$\Delta\rho_{max}/\Delta\rho_{min,}$ (e Å^{-3})	0.96/−0.76	1.84/−2.12
Flack	0.023(7)	0.001(12)

$^aR = \Sigma||F_o|-|F_c||/\Sigma|F_o|$, $^bwR = (\Sigma(w(F_o{}^2-F_c{}^2)^2)/\Sigma(w(F_o{}^2)^2))^{1/2}$.

Table S2. Coordinates, equivalent isotropic displacement parameters, and bond valence sum of all crystallographically independent atoms in **1**–**6**.

1					
atoms	x	y	z	U(eq)	BV
K1	0.7556(5)	0.2218(4)	0.0148(5)	0.0940(17)	0.4462
K2	0.0840(4)	0.8274(3)	0.7596(3)	0.0581(10)	0.7778
K3	0.7866(4)	0.9040(3)	0.4338(3)	0.0535(10)	0.8246
K4	0.1144(4)	0.6036(3)	0.4174(3)	0.0632(10)	0.8989
K5	0.6375(4)	0.5644(3)	0.5974(3)	0.0628(11)	0.8664
Cl1	0.9108(4)	0.7213(3)	0.5483(3)	0.0377(8)	−1.0880
In1	0.42052(11)	0.63980(8)	0.90462(8)	0.0206(2)	3.0198
In2	0.71336(10)	0.20834(8)	0.63690(8)	0.0208(2)	2.9889
In3	0.62935(10)	0.56899(8)	0.20891(8)	0.0204(2)	3.0606
In4	0.56274(10)	0.93515(7)	0.76196(7)	0.0202(2)	3.0125
In5	0.35516(10)	0.99405(8)	0.48726(7)	0.0191(2)	3.0394
In6	0.78119(10)	0.86530(8)	0.05654(7)	0.0193(2)	3.0069
In7	0.40412(11)	0.82048(8)	0.19915(8)	0.0216(2)	3.0620
In8	0.10825(11)	0.24821(9)	0.47195(8)	0.0217(2)	3.0483
In9	0.34040(10)	0.18067(8)	0.77254(7)	0.0221(2)	2.9613
In10	0.07651(10)	0.43922(7)	0.76671(7)	0.0201(3)	3.0361
In11	0.26719(10)	0.36032(8)	0.06009(7)	0.0200(2)	2.9616
In12	0.12524(10)	0.06762(8)	0.19128(7)	0.0200(3)	2.9875
In13	0.02065(11)	0.59205(8)	0.04574(8)	0.0219(2)	3.0036
In14	0.49102(10)	0.29639(8)	0.34211(7)	0.0202(2)	3.0612
Se1	0.66301(13)	0.76861(10)	0.86417(9)	0.0176(3)	−2.0365
Se2	0.58717(13)	0.12882(10)	0.43853(10)	0.0189(3)	−2.1324
Se3	0.92875(13)	0.35956(11)	0.57773(10)	0.0178(3)	−2.0413
Se4	0.24629(14)	0.74899(12)	0.01206(11)	0.0217(3)	−2.1328
Se5	0.56706(16)	0.32550(11)	0.75226(12)	0.0332(3)	−1.8761
Se6	0.87067(14)	0.70755(11)	0.17405(10)	0.0183(3)	−2.0251
Se7	0.62170(14)	0.96994(11)	0.17323(10)	0.0257(3)	−1.8975
Se8	0.20048(13)	0.90319(10)	0.30602(9)	0.0180(3)	−2.0494
Se9	0.51511(14)	0.48019(10)	0.01193(10)	0.0203(3)	−2.0570
Se10	0.29712(14)	0.57496(12)	0.71403(10)	0.0288(3)	−1.9244
Se11	0.16695(14)	0.08677(11)	0.59669(10)	0.0213(3)	−2.0768
Se12	0.88455(15)	0.53710(14)	0.85704(12)	0.0403(4)	−1.8201
Se13	0.46936(16)	0.67205(12)	0.32516(11)	0.0321(3)	−1.9524
Se14	0.81260(14)	0.04537(12)	0.72058(12)	0.0350(4)	−1.7990
Se15	0.94410(14)	0.15016(12)	0.30725(11)	0.0262(3)	−1.8632
Se16	0.00000(14)	0.00000(12)	0.00000(10)	0.0251(3)	−1.8181
Se17	0.73445(14)	0.41363(12)	0.30265(12)	0.0321(4)	−1.8011
Se18	0.42325(17)	0.82945(11)	0.58579(11)	0.0322(4)	−1.8161
Se19	0.39751(17)	0.02290(12)	0.88946(11)	0.0316(3)	−1.8121
Se20	0.13122(14)	0.26615(10)	0.87281(10)	0.0195(3)	−2.0356
Se21	0.37376(13)	0.19582(10)	0.15131(9)	0.0185(3)	−2.0443
Se22	0.07178(17)	0.43487(12)	0.16519(11)	0.0321(3)	−1.9052
Se23	0.32914(15)	0.39879(11)	0.45699(11)	0.0284(3)	−2.0591
2					
atoms	x	y	z	U(eq)	BV
Rb1	0.79041(17)	0.90835(12)	0.42885(13)	0.0416(3)	0.9620
Rb2	0.11753(17)	0.60516(14)	0.41089(13)	0.0471(4)	1.0488
Rb3	0.7547(2)	0.22858(16)	0.01089(17)	0.0579(5)	0.5311
Rb4	0.08247(17)	0.83365(14)	0.76398(12)	0.0440(3)	0.9335
Rb5	0.63239(17)	0.56673(14)	0.59646(13)	0.0470(4)	1.0138
Cl1	0.9138(3)	0.7229(3)	0.5474(3)	0.0348(7)	−1.2969

In1	0.41958(10)	0.64113(7)	0.90269(7)	0.0186(2)	2.9634
In2	0.63040(9)	0.56954(7)	0.20445(7)	0.0186(2)	2.9948
In3	0.35654(9)	0.99594(7)	0.48499(7)	0.0177(2)	2.9772
In4	0.56316(9)	0.93766(7)	0.75989(7)	0.0185(2)	2.9446
In5	0.71228(9)	0.20971(8)	0.63386(7)	0.01916(19)	2.9412
In6	0.49010(9)	0.29730(7)	0.33831(7)	0.0184(2)	3.0140
In7	0.78081(9)	0.86598(7)	0.05382(7)	0.0179(2)	2.9580
In8	0.40629(9)	0.82206(7)	0.19686(7)	0.0193(2)	3.0104
In9	0.10802(10)	0.24823(8)	0.46985(7)	0.0195(2)	3.0003
In10	0.34037(9)	0.18122(7)	0.76852(7)	0.0198(2)	2.9235
In11	0.26822(9)	0.36052(7)	0.05586(7)	0.0181(2)	2.9138
In12	0.12601(9)	0.06913(7)	0.18989(7)	0.0179(2)	2.9358
In13	0.07477(9)	0.43923(7)	0.76499(7)	0.0181(2)	2.9787
In14	0.02200(9)	0.59222(7)	0.04286(7)	0.01935(19)	2.9511
Se1	0.58639(12)	0.13109(10)	0.43621(10)	0.0175(2)	−2.1126
Se2	0.87043(12)	0.70762(10)	0.16918(10)	0.0166(2)	−1.9860
Se3	0.24722(14)	0.74895(11)	0.01200(10)	0.0198(3)	−2.1226
Se4	0.20421(12)	0.90559(10)	0.30362(9)	0.0163(3)	−2.0101
Se5	0.66057(12)	0.77024(9)	0.86232(9)	0.0162(2)	−1.9924
Se6	0.92950(12)	0.35889(10)	0.57626(9)	0.0160(2)	−1.9937
Se7	0.51419(12)	0.48139(10)	0.00854(9)	0.0186(3)	−2.0238
Se8	0.61947(13)	0.97137(10)	0.16621(10)	0.0234(3)	−1.8936
Se9	0.56444(14)	0.32577(11)	0.74741(11)	0.0283(3)	−1.8965
Se10	0.16758(13)	0.08718(10)	0.59325(10)	0.0189(3)	−2.0546
Se11	0.88225(14)	0.53301(13)	0.85752(12)	0.0339(4)	−1.8033
Se12	0.94635(13)	0.15470(11)	0.30300(10)	0.0235(3)	−1.8583
Se13	0.47519(15)	0.67468(11)	0.32167(11)	0.0274(3)	−1.9548
Se14	0.32874(14)	0.39670(11)	0.45439(11)	0.0266(3)	−2.0942
Se15	0.81151(13)	0.04957(11)	0.72112(11)	0.0297(3)	−1.7896
Se16	0.29188(14)	0.57736(11)	0.71448(10)	0.0265(3)	−1.9379
Se17	0.00004(13)	0.00004(11)	0.00043(9)	0.0222(3)	−1.8397
Se18	0.13372(12)	0.26667(9)	0.86936(9)	0.0174(3)	−2.0072
Se19	0.73181(13)	0.41343(11)	0.29802(12)	0.0281(3)	−1.7875
Se20	0.37274(12)	0.19663(9)	0.14852(9)	0.0170(2)	−2.0079
Se21	0.40099(15)	0.02672(11)	0.88724(10)	0.0257(3)	−1.8198
Se22	0.42516(15)	0.83238(10)	0.58391(10)	0.0271(3)	−1.7948
Se23	0.07488(15)	0.43524(11)	0.16086(11)	0.0276(3)	−1.9182

3

atoms	x	y	z	U(eq)	BV
Ba1	1	1	0.99679(9)	0.0515(5)	1.4152
K1	0.7903(3)	0.7903(3)	0.8026(2)	0.0683(12)	0.9018
K2	0.66667	0.33333	0.9459(3)	0.089(2)	0.4021
Cl1	1	1	0.8445(3)	0.0342(15)	−1.1484
In1	0.82891(5)	0.49119(5)	0.75973(4)	0.02152(17)	3.0117
In2	0.84206(6)	0.67456(5)	0.58570(4)	0.02224(17)	2.9846
In3	1	0.50319(7)	1.08364(5)	0.0216(2)	3.0035
In4	1	0.66770(7)	0.92911(5)	0.0224(2)	3.0793
Se1	1	0.68051(9)	0.79396(6)	0.0175(3)	−1.9914
Se2	0.81930(7)	0.48629(7)	0.62597(5)	0.0211(2)	−2.0230
Se3	1	0.84859(10)	0.63750(7)	0.0276(3)	−1.8215
Se4	0.9719(2)	0.47950(18)	0.95735(9)	0.0370(9)	−1.8326
Se5	0.8417(3)	0.7014(3)	0.95928(12)	0.0447(8)	−1.9670
Se5A	0.8092(4)	0.6373(5)	0.9574(2)	0.0447(8)	−1.9670
Se6	0.67097(8)	0.51083(8)	0.80637(6)	0.0308(3)	−1.9397
Se7	1	0.66998(9)	1.14277(6)	0.0186(3)	−2.0842

4

atoms	x	y	z	U(eq)	BV

Ba1	1	1	0.99968(8)	0.0500(4)	1.4235
Rb1	1.20823(10)	1	0.79849(9)	0.0466(3)	1.0494
Rb2	0.66667	0.33333	0.95067(11)	0.0605(6)	0.3474
Cl1	1	1	0.8504(2)	0.0294(11)	−1.3749
In1	0.82848(4)	0.49138(4)	0.75966(3)	0.02018(16)	2.9663
In2	0.84177(4)	0.67432(4)	0.58550(3)	0.02080(15)	2.9404
In3	1	0.50222(5)	1.08300(4)	0.01987(19)	2.5208
In4	1	0.66783(6)	0.92952(4)	0.0214(2)	2.5912
Se1	1	0.67965(7)	0.79458(6)	0.0174(2)	−1.9587
Se2	0.81991(7)	0.48702(6)	0.62613(4)	0.01948(19)	−1.9835
Se3	0.84763(9)	0.84763(9)	1.13786(7)	0.0260(3)	−1.7761
Se4	1	0.4918(9)	0.9558(8)	0.031(5)	−1.8243
Se4A	1.029(5)	0.509(2)	0.9579(4)	0.031(5)	−1.8243
Se5	0.8120(4)	0.6451(4)	0.9568(2)	0.0395(7)	−1.9422
Se5A	0.8404(2)	0.6987(3)	0.95968(12)	0.0395(7)	−1.9422
Se6	0.67023(6)	0.51000(7)	0.80567(5)	0.0273(2)	−1.9455
Se7	1	0.66904(7)	1.14117(6)	0.0177(2)	−2.0911

5

atoms	x	y	z	U(eq)	BV
Li1	0.0000	0.002(2)	0.0000	0.029(5)	1.0838
K1	0.18033(9)	0.0063(2)	0.10327(11)	0.0339(5)	1.2292
K2	0.36302(11)	0.2271(3)	0.08087(14)	0.0582(8)	0.5713
K3	0.09441(10)	0.2586(2)	0.65470(12)	0.0455(6)	0.7611
K4	0.0000	0.6823(3)	0.0000	0.0392(8)	1.1759
K5	0.02086(9)	0.0127(2)	0.19546(11)	0.0364(5)	1.2264
K6	0.0000	0.3239(3)	0.0000	0.0398(8)	1.2368
K7	0.42782(12)	0.4839(3)	0.54665(15)	0.0580(8)	0.8346
K8	0.17436(11)	0.2976(3)	0.24654(13)	0.0554(7)	0.6616
Cl1	0.0000	0.1279(4)	0.5000	0.0407(9)	−1.0454
Cl2	0.07619(9)	0.1227(2)	0.11171(12)	0.0288(5)	−1.1827
Cl3	0.44257(9)	0.3840(2)	0.03547(11)	0.0300(6)	−1.1331
In1	0.47604(3)	0.13167(7)	0.33466(3)	0.01947(15)	3.0397
In2	0.59125(3)	0.13542(7)	0.26761(3)	0.01926(16)	3.0833
In3	0.03774(3)	0.38700(8)	0.80440(3)	0.01941(16)	3.0708
In4	0.11219(3)	0.38173(6)	0.41847(3)	0.01778(16)	3.0768
In5	0.21467(3)	0.62559(7)	0.19092(3)	0.01874(15)	3.0466
In6	0.36147(3)	0.13020(6)	0.41787(3)	0.01930(16)	3.0307
In7	0.32503(3)	0.62582(7)	0.11658(3)	0.01846(15)	3.0626
In8	0.25072(3)	0.13956(7)	0.48931(4)	0.01941(16)	3.0704
In9	0.34277(3)	0.39127(7)	0.26522(3)	0.01803(16)	3.0812
In10	0.19508(3)	0.38559(7)	0.04242(3)	0.01882(16)	3.0825
In11	0.26893(3)	0.38916(7)	0.65330(3)	0.01880(16)	3.0488
Se1	0.05038(4)	0.49890(9)	0.46227(5)	0.0190(2)	−2.0089
Se2	0.43004(4)	0.26893(8)	0.39304(5)	0.0157(2)	−2.0029
Se3	0.02378(5)	0.49738(11)	0.15091(6)	0.0390(3)	−1.9890
Se4	0.64645(4)	0.26780(9)	0.21909(5)	0.0162(2)	−1.9561
Se5	0.17973(4)	0.50366(9)	0.38504(5)	0.0187(2)	−2.1434
Se6	0.39188(4)	0.00436(11)	0.22204(5)	0.0286(2)	−1.9133
Se7	0.12672(4)	0.50383(10)	0.07322(6)	0.0340(3)	−2.0061
Se8	0.03605(4)	0.24330(11)	0.30887(5)	0.0357(3)	−1.9579
Se9	0.53467(5)	0.27435(11)	0.30313(6)	0.0320(3)	−1.9931
Se10	0.39046(4)	0.74458(9)	0.07358(4)	0.0158(2)	−1.9517
Se11	0.29178(4)	0.51276(10)	0.31954(5)	0.0264(2)	−1.8628
Se12	0.18787(4)	0.24419(9)	0.53881(5)	0.0174(2)	−2.0788
Se13	0.20287(4)	0.48514(10)	0.69512(5)	0.0266(2)	−1.9754
Se14	0.41313(4)	0.51309(10)	0.24003(6)	0.0298(3)	−1.9407
Se15	0.76658(4)	0.26842(10)	0.14927(5)	0.0270(2)	−2.0416

Se16	0.30539(4)	0.27667(10)	0.45030(6)	0.0277(2)	−1.9948
Se17	0.16483(4)	0.01162(11)	0.37633(6)	0.0319(3)	−2.0051
Se18	0.25020(5)	0.00356(10)	0.00765(6)	0.0304(3)	−2.0452
Se19	0.26891(4)	0.24523(10)	0.15627(5)	0.0291(2)	−2.0206
			6		
atoms	x	y	z	U(eq)	BV
K1	0.82223(17)	0.9945(3)	0.8977(2)	0.0650(9)	0.7438
Ba1	0.82223(17)	0.9945(3)	0.8977(2)	0.0650(9)	1.1955
K2	0.63979(14)	0.7788(3)	0.91874(19)	0.0572(9)	0.7502
Ba2	0.63979(14)	0.7788(3)	0.91874(19)	0.0572(9)	1.1695
K3	0.9059(2)	0.7416(4)	0.3453(3)	0.0456(11)	1.1087
K4	1	0.3054(6)	1	0.0462(17)	1.1039
K5	0.9788(2)	0.9874(4)	0.8121(3)	0.0446(11)	1.1194
K6	1	0.6882(7)	1	0.0491(17)	1.1293
K7	0.5724(3)	0.5154(5)	0.4520(4)	0.0619(15)	0.8184
K8	0.8228(2)	0.6928(5)	0.7488(3)	0.0603(14)	0.8135
Cl1	1	0.8736(7)	0.5	0.0392(16)	−0.9885
Cl2	0.9121(2)	0.8626(5)	0.8736(3)	0.0399(11)	−1.0935
Cl3	0.5664(2)	0.6317(5)	0.9603(3)	0.0425(12)	−1.1018
In1	0.52319(5)	0.86863(13)	0.66490(7)	0.0207(3)	2.9889
In2	0.40963(5)	0.86372(12)	0.73382(7)	0.0208(3)	3.0202
In3	1.03681(5)	0.61403(14)	0.80464(6)	0.0209(3)	2.9846
In4	0.88792(5)	0.61854(12)	0.58196(6)	0.0194(3)	3.0133
In5	0.78509(5)	0.37258(12)	0.81034(7)	0.0204(3)	2.9710
In6	0.63845(5)	0.87029(11)	0.58248(6)	0.0211(3)	2.9486
In7	0.67386(5)	0.37549(12)	0.88330(7)	0.0201(3)	2.9985
In8	0.74906(6)	0.86014(11)	0.51085(7)	0.0211(3)	3.0183
In9	0.65630(5)	0.60810(12)	0.73433(7)	0.0194(3)	3.0127
In10	0.80541(6)	0.61487(12)	0.95689(7)	0.0205(3)	3.0192
In11	0.73114(5)	0.60970(12)	0.34646(6)	0.0205(3)	2.9810
Se1	0.94952(8)	0.50162(16)	0.53775(9)	0.0203(4)	−1.9833
Se2	0.56975(7)	0.73150(15)	0.60697(9)	0.0172(4)	−1.9564
Se3	0.97709(11)	0.5014(2)	0.85072(12)	0.0411(6)	−1.9195
Se4	0.35318(7)	0.73186(16)	0.78116(9)	0.0179(4)	−1.9328
Se5	0.82106(8)	0.49510(16)	0.61564(10)	0.0195(4)	−2.1182
Se6	0.60742(8)	0.99665(19)	0.77774(11)	0.0284(4)	−1.8877
Se7	0.87379(9)	0.49316(19)	0.92824(13)	0.0376(5)	−1.9149
Se8	0.96394(9)	0.75775(19)	0.69129(10)	0.0349(5)	−1.8897
Se9	0.46647(10)	0.7250(2)	0.69855(12)	0.0350(5)	−1.9455
Se10	0.60944(7)	0.25615(16)	0.92712(9)	0.0171(4)	−1.9119
Se11	0.70650(9)	0.48298(18)	0.68057(10)	0.0279(4)	−1.8294
Se12	0.81180(8)	0.75560(16)	0.46139(10)	0.0183(4)	−2.0275
Se13	0.79801(9)	0.51678(18)	0.30488(10)	0.0270(4)	−1.9181
Se14	0.58583(9)	0.48956(19)	0.76104(12)	0.0337(5)	−1.8785
Se15	0.73296(9)	1.23135(18)	0.85278(11)	0.0299(5)	−1.9848
Se16	0.69318(9)	0.72326(17)	0.54848(12)	0.0303(5)	−1.9653
Se17	0.83499(9)	0.9886(2)	0.62318(12)	0.0330(5)	−1.9645
Se18	0.75091(10)	1.00033(18)	0.99309(12)	0.0316(4)	−2.0124
Se19	0.73079(8)	0.75491(18)	0.84297(10)	0.0285(5)	−1.9935

Table S3. Selected bond lengths [Å] for **1**–**6**.

1			
Bonds	Distances	Bonds	Distances
Cl1-K2	3.012(5)	In7-Se8	2.6242(16)
Cl1-K3	2.994(5)	In7-Se13	2.5320(17)
Cl1-K4	2.995(5)	In8-Se3	2.6303(15)
Cl1-K5	3.003(5)	In8-Se11	2.6309(14)
In1-Se1	2.5900(14)	In8-Se15	2.5192(14)
In1-Se4	2.5906(17)	In8-Se23	2.5185(15)
In1-Se9	2.6049(15)	In9-Se5	2.5262(16)
In1-Se10	2.5171(14)	In9-Se11	2.6409(14)
In2-Se2	2.6455(12)	In9-Se19	2.5346(16)
In2-Se3	2.6361(14)	In9-Se20	2.6396(16)
In2-Se5	2.5249(16)	In10-Se3	2.6187(13)
In2-Se14	2.5230(16)	In10-Se10	2.5334(15)
In3-Se6	2.6226(14)	In10-Se12	2.5337(17)
In3-Se9	2.6310(14)	In10-Se20	2.6113(15)
In3-Se13	2.5153(16)	In11-Se9	2.6072(15)
In3-Se17	2.5229(16)	In11-Se20	2.6122(13)
In4-Se1	2.6649(14)	In11-Se21	2.6080(14)
In4-Se14	2.5473(16)	In11-Se22	2.5083(17)
In4-Se18	2.5654(14)	In12-Se8	2.6361(15)
In4-Se19	2.5356(16)	In12-Se15	2.5259(17)
In5-Se2	2.5855(14)	In12-Se16	2.5365(14)
In5-Se8	2.6051(13)	In12-Se21	2.6273(14)
In5-Se11	2.5900(15)	In13-Se4	2.6436(14)
In5-Se18	2.5130(16)	In13-Se6	2.6262(16)
In6-Se1	2.6237(13)	In13-Se12	2.5181(15)
In6-Se6	2.6347(13)	In13-Se22	2.5324(17)
In6-Se7	2.5258(16)	In14-Se2	2.6266(14)
In6-Se16	2.5318(15)	In14-Se17	2.5286(16)
In7-Se4	2.6156(14)	In14-Se21	2.6218(13)
In7-Se7	2.5163(15)	In14-Se23	2.5134(17)
2			
Bonds	Distances	Bonds	Distances
Cl1-Rb1	3.060(4)	In7-Se8	2.5313(14)
Cl1-Rb2	3.057(3)	In7-Se17	2.5347(14)
Cl1-Rb2	3.056(3)	In8-Se3	2.6198(13)
Cl1-Rb4	3.083(3)	In8-Se4	2.6370(14)
In1-Se3	2.5996(14)	In8-Se8	2.5188(15)
In1-Se5	2.5999(13)	In8-Se13	2.5388(16)
In1-Se7	2.6129(14)	In9-Se6	2.6420(13)
In1-Se16	2.5192(13)	In9-Se10	2.6355(14)
In2-Se2	2.6310(13)	In9-Se12	2.5260(13)
In2-Se7	2.6391(13)	In9-Se14	2.5201(15)
In2-Se13	2.5243(14)	In10-Se9	2.5271(15)
In2-Se19	2.5298(15)	In10-Se10	2.6503(13)
In3-Se1	2.5927(14)	In10-Se18	2.6445(14)
In3-Se4	2.6124(13)	In10-Se21	2.5397(15)
In3-Se10	2.5980(13)	In11-Se7	2.6150(14)
In3-Se22	2.5210(15)	In11-Se18	2.6151(12)
In4-Se5	2.6804(13)	In11-Se20	2.6168(12)
In4-Se15	2.5545(15)	In11-Se23	2.5131(14)
In4-Se21	2.5413(14)	In12-Se4	2.6456(14)
In4-Se22	2.5728(13)	In12-Se12	2.5322(15)
In5-Se1	2.6515(12)	In12-Se17	2.5399(13)
In5-Se6	2.6438(14)	In12-Se20	2.6349(13)
In5-Se9	2.5312(14)	In13-Se6-	2.6264(12)

In5-Se15	2.5274(14)	In13-Se11	2.5424(15)
In6-Se1	2.6373(14)	In13-Se16	2.5358(14)
In6-Se14	2.5168(15)	In13-Se18	2.6214(14)
In6-Se19	2.5321(15)	In14-Se2	2.6388(13)
In6-Se20	2.6286(13)	In14-Se3	2.6489(14)
In7-Se2	2.6429(12)	In14-Se11	2.5206(14)
In7-Se5	2.6327(13)	In14-Se23	2.5394(16)
3			
Bonds	Distances	Bonds	Distances
Cl1-K1×3	3.050(4)	In2-Se7	2.6304(10)
Cl1-Ba1	2.997(6)	In3-Se2	2.5974(11)
In1-Se1	2.6213(10)	In3-Se4	2.513(2)
In1-Se2	2.6356(11)	In3-Se4	2.5129(19)
In1-Se6	2.5335(12)	In3-Se7	2.6098(15)
In1-Se6	2.5242(11)	In4-Se1	2.6665(15)
In2-Se2	2.6154(11)	In4-Se4	2.524(2)
In2-Se3	2.5457(11)	In4-Se4	2.524(2)
In2-Se5	2.510(3)	In4-Se5	2.557(3)
In2-Se5A	2.566(4)	In4-Se5A	2.548(5)
4			
Bonds	Distances	Bonds	Distances
Cl1-Rb1×3	3.104(2)	In2-Se7	2.6347(9)
Cl1-Ba1	2.953(5)	In3-Se2×2	2.6050(9)
In1-Se1	2.6313(9)	In3-Se4	2.520(16)
In1-Se2	2.6431(10)	In3-Se4A	2.502(15)
In1-Se6	2.5266(9)	In3-Se7	2.6136(13)
In1-Se6	2.5369(9)	In4-Se1	2.6739(14)
In2-Se2	2.6215(9)	In4-Se4	2.531(10)
In2-Se3	2.5582(10)	In4-Se4A	2.536(13)
In2-Se5	2.572(4)	In4-Se5×2	2.557(5)
In2-Se5A	2.507(3)	In4-Se5A	2.562(3)
5			
Bonds	Distances	Bonds	Distances
Cl3-Li1×2	2.385(14)	In5-Se15	2.5363(11)
Cl2-Li1×2	2.401(14)	In5-Se11	2.5378(11)
Cl1-K3×2	3.032(3)	In5-Se7	2.5520(11)
Cl1-K7×2	3.000(3)	In5-Se4	2.6734(10)
Cl2-K1×2	3.059(3)	In6-Se16	2.5255(11)
Cl2-K5×2	3.034(3)	In6-Se13	2.5278(11)
Cl2-K6×2	3.030(4)	In6-Se2	2.6168(10)
Cl2-K8×2	3.145(3)	In6-Se1	2.6339(11)
Cl3-K1×2	3.088(3)	In7-Se18	2.5360(12)
Cl3-K2×2	3.215(3)	In7-Se15	2.5431(11)
Cl3-K5×2	3.040(3)	In7-Se14	2.5512(11)
Cl3-K4×2	3.038(4)	In7-Se10	2.6574(10)
In1-Se6	2.5122(11)	In8-Se16	2.5114(11)
In1-Se9	2.5332(12)	In8-Se17	2.5341(12)
In1-Se2	2.6174(10)	In8-Se12	2.6177(10)
In1-Se1	2.6393(11)	In8-Se5-	2.6211(11)
In2-Se9	2.5160(11)	In9-Se19	2.5394(12)
In2-Se3	2.5269(11)	In9-Se14	2.5447(11)
In2-Se4	2.6156(10)	In9-Se11	2.5467(11)
In2-Se5	2.6191(11)	In9-Se2	2.6455(10)
In3-Se6	2.5327(11)	In10-Se18	2.5360(11)
In3-Se3	2.5513(11)	In10-Se19	2.5430(11)
In3-Se8	2.5617(12)	In10-Se7	2.5512(10)
In3-Se10	2.6332(10)	In10-Se10	2.6459(11)

In4-Se8	2.5032(11)	In11-Se17	2.5186(11)
In4-Se1	2.5844(10)	In11-Se13	2.5291(10)
In4-Se5	2.5909(10)	In11-Se4	2.6196(10)
In4-Se12	2.5982(11)	In11-Se12	2.6279(11)
6			
Bonds	Distances	Bonds	Distances
Cl1-K3×2	3.045(6)	In5-Se7	2.561(2)
Cl1-K7×2	3.019(7)	In5-Se11	2.551(2)
Cl2-K1/Ba1	3.020(6)	In5-Se15	2.546(2)
Cl2-K5	2.997(6)	In6-Se1	2.644(2)
Cl2-K6	3.006(7)	In6-Se2	2.6248(19)
Cl2-K8	2.968(7)	In6-Se13	2.539(2)
Cl3-K1/Ba1	3.078(6)	In6-Se16	2.532(2)
Cl3-K2/Ba2	2.989(6)	In7-Se10	2.6604(19)
Cl3-K4	3.017(7)	In7-Se14	2.555(2)
Cl3-K5	3.015(7)	In7-Se15	2.549(2)
In1-Se1	2.640(2)	In7-Se18	2.552(2)
In1-Se2	2.6278(19)	In8-Se5	2.633(2)
In1-Se6	2.527(2)	In8-Se12	2.6235(19)
In1-Se9	2.539(2)	In8-Se16	2.523(2)
In2-Se3	2.533(2)	In8-Se17	2.540(2)
In2-Se4	2.6283(19)	In9-Se2	2.650(2)
In2-Se5	2.632(2)	In9-Se11	2.555(2)
In2-Se9	2.524(2)	In9-Se14	2.555(2)
In3-Se3	2.556(2)	In9-Se19	2.553(2)
In3-Se6	2.553(2)	In10-Se7	2.555(2)
In3-Se8	2.565(2)	In10-Se10	2.653(2)
In3-Se10	2.646(2)	In10-Se18	2.555(2)
In4-Se1	2.5933(19)	In10-Se19	2.553(2)
In4-Se5	2.599(2)	In11-Se4	2.630(2)
In4-Se8	2.513(2)	In11-Se12	2.643(2)
In4-Se12	2.606(2)	In11-Se13	2.537(2)
In5-Se4	2.6820(19)	In11-Se17	2.526(2)

Table S4. A summary of phase-matching SICs and their SHG intensities.

Formula	SHG (× AGS)	Formula	SHG (×
$[Sr_4Cl_2][Si_3S_9]$[10]	1.2	$[Na_2PbI][Ga_7S_{12}]$[18]	2.6
$[K_3Cl][Ga_3PS_8]$[11]	1	$[K_4Cl][CdGa_9S_{16}]$[19]	0.9
$[Rb_3Cl][Ga_3PS_8]$[11]	1.1	$[K_4Cl][CdGa_9Se_{16}]$[19]	2.4
$[K_3Br][Ga_3PS_8]$[11]	1.2	$[K_4Cl][MnGa_9S_{16}]$[20]	0.6
$[Rb_3Br][Ga_3PS_8]$[11]	2	$[K_4Cl][HgGa_9S_{16}]$[20]	1
$[RbBa_2Cl][Ga_4S_8]$[12]	1	$[K_3Cl][Mn_2Ga_6S_{12}]$[21]	0.8
$[CsBa_2Cl][Ga_4S_8]$[12]	0.9	$Rb_6[K_3Cl][Li_2Mn_4Ga_{12}S_{27}]$[22]	1.1
$Li[LiCs_2Cl][Ga_3S_6]$[13]	0.7	$[CsBa_3Br][B_2S_6]$[23]	0.5
$[Ba_4Cl_2][ZnGa_4S_{10}]$[14]	1.1	$[CsBa_3I][B_2S_6]$[23]	0.5
$[Ba_4Cl_2][HgGa_4S_{10}]$[15]	1.5	$[RbBa_3Br][B_2S_6]$[23]	0.6
$[KBa_3Cl_2][Ga_5S_{10}]$[16]	1	$[RbBa_3I][B_2S_6]$[23]	0.5

$[RbBa_3Cl_2][Ga_5S_{10}]$[16]	1	$[RbBa_3Cl][In_8Se_{14}]$[24]	2.0
$[CsBa_3Cl_2][Ga_5S_{10}]$[16]	1	$[Na_4I][Ga_9S_{15}]$[25]	0.7
$[K_2PbCl][Ga_7S_{12}]$[17]	2.5	**$[K_4Cl][LiK_{10}Cl_4][In_{22}Se_{38}]$** **this work**	2.0
$[K_2PbBr][Ga_7S_{12}]$[17]	2.6	**$[K_4Cl][BaK_9Cl_4][In_{22}Se_{38}]$** **this work**	2.1
$[K_2PbI][Ga_7S_{12}]$[17]	2.7		

Table S5. Thermal expansion coefficients (α_L) of **1**−**6** and benchmark AGS along the *a*-, *b*-, and *c*-axis, separately.

Compounds	α_L ($\times 10^{-5}$)		
	a-axis	*b*-axis	*c*-axis
AGS	3.080	3.080	–9.158
1	1.925	1.408	1.796
2	1.733	1.475	2.147
3	2.320	2.320	1.079
4	1.755	1.755	1.466
5	0.720	1.359	1.304
6	1.037	1.403	1.481

Table S6. The laser-induced damage thresholds (LIDTs) of **1**−**6** and $AgGaS_2$ determined by single crystals.

Compounds	Incidence laser wavelength (nm)	Damage energy (mJ)	Spot area (cm^2)	τp (ns)	Damage threshold [$MW \cdot cm^{-2}$]
AGS	1064	0.80	0.020	10	4.0
1	1064	3.30	0.020	10	16.5
2	1064	2.90	0.020	10	14.5
3	1064	2.70	0.020	10	13.5
4	1064	2.46	0.020	10	12.3
5	1064	3.44	0.020	10	17.2
6	1064	3.12	0.020	10	15.6

References

[1] (a) G. Sheldrick, SHELXS-97: Program for X-Ray Crystal Structure Solution; University of Gö Ttingen: Gö Ttingen; Germany, 1997. (b) Rigaku Oxford Diffraction, Crysalispro Software System, Version V40.67a; Rigaku Corporation; Oxford, UK, 2019.

[2] G. Korum, Reflectance Spectroscopy, Springer: New York, 1969.

[3] S. Kurtz, and T. Perry, *J. Appl. Phys.* 1968, **39**, 3798−3813.

[4] I. D. Brown, The Chemical Bond in Inorganic Chemistry: The Bond Valence Model. Oxford University Press, 2002.

[5] R. Nelson, C. Ertural, J. George, et al. *J. Comput. Chem.* 2020, **41**, 1931–1940.

[6] (a) S. Clark, M. Segall, C. Pickard, et al. *Z. Kristallogr. Cryst. Mater.* 2005, **220**, 567–570. (b) X. Gonze, B. Amadon, G. Antonius, et al. *Comput. Phys. Commun.* 2019, **248**, 107042.

[7] J. Perdew, J. Chevary, S. Vosko, et al. *Phys. Rev. B* 1992, **46**, 6671–6687.

[8] S. Baroni, S. Gironcoli, A. Corso, et al. *Rev. Mod. Phys.* 2001, **73**, 515−562.

[9] S. Sharma, and C. Ambrosch-Draxl, *Phys. Scr.* 2004, **T109**, 128–134.

[10] C. Zhao, K. Wu, Y. Xiao, B. Zhang, H. Yu, and H. Zhang, *J. Mater. Chem. C* 2023, **11**, 4439–4443.

[11] B.-W. Liu, H.-Y. Zeng, X.-M. Jiang, G.-E. Wang, S.-F. Li, L. Xu, and G.-C. Guo, *Chem. Sci.* 2016, **7**, 6273–6277.

[12] B.-W. Liu, X.-M. Jiang, H.-Y. Zeng, and G.-C. Guo, *J. Am. Chem. Soc.* 2020, **142**, 10641−10645.

[13] B.-W. Liu, X.-M. Jiang, B.-X. Li, H.-Y. Zeng, and G.-C. Guo, *Angew. Chem. Int. Ed.* 2020, **59**, 4856–4859.

[14] H. Chen, Y. Y. Li, B. Li, P. F. Liu, H. Lin, Q. L. Zhu, and X. T. Wu, *Chem. Mater.* 2020, **32**, 8012–8019.

[15] Y. Zhang, H. Wu, Z. Hu, J. Wang, Y. Wu, and H. Yu, *Inorg. Chem. Front.* 2022, **9**, 4075–4080.

[16] B.-W. Liu, H.-Y. Zeng, X.-M. Jiang, and G.-C. Guo, *CCS Chem.* 2020, **3**, 964–973.

[17] W.-F. Chen, B.-W. Liu, S.-M. Pei, X.-M. Jiang, G.-C. Guo, *Adv. Sci.* 2023, **10**, 2207630.

[18] Z.-X. Wu, W.-F. Chen, X.-M. Jiang, B.-W. Liu, G.-C. Guo, *Chem. Mater.* 2024, **36**, 3444−3451.

[19] S.-M. Pei, B.-W. Liu, X.-M. Jiang, Y.-Q. Zou, W.-F. Chen, Q.-N. Yan, and G.-C. Guo, *Chem. Mater.* 2021, **33**, 8831–8837.

[20] S.-M. Pei, M.-S. Zhang, F. Wu, Y. Guo, B.-W. Liu, X.-M. Jiang, and G.-C. Guo, *Chem. Sci.* 2024, **15**, 13753−13759.

[21] B.-W. Liu, S.-M. Pei, X.-M. Jiang, and G.-C. Guo, *Mater. Horiz.* 2022, **9**, 1513–1517.

[22] S.-M. Pei, B.-W. Liu, W.-F. Chen, X.-M. Jiang, and G.-C. Guo, *Mater. Horiz.* 2023, **10**, 2921–2926.

[23] J. Zhou, K. Hou, Y. Chu, Z. Yang, J. Li, and S. Pan, Small 2024, **20**, 2308806.

[24] F. Wu, W.-F. Chen, Z.-X. Wu, X.-M. Jiang, B.-W. Liu, and G.-C. Guo, *Sci. China Mater.* 2024, **67**, 2000–2007.

[25] Y. Guo, W.-F. Chen, M.-X. Li, F. Wu, Q.-P. Qin, B.-W. Liu, X.-M. Jiang, G.-C. Guo, *Chem. Mater.* 2024, **36**, 4838−4848.